Single Crystal Investigation and Physical Properties of the Binary Compound CeB_4

Volodymyr Babizhetskyy[a], Arndt Simon[a], and Kurt Hiebl[b]

[a] Max-Planck Institut für Festkörperforschung, Heisenbergstraße 1, D-70569 Stuttgart, Germany
[b] Arbeitsgruppe Neue Materialien, Universität Wien, Währingerstraße 42, A-1090 Wien, Austria

Reprint requests to K. Hiebl. E-mail: Kurt.Hiebl@univie.ac.at

Z. Naturforsch. **2007**, *62b,* 896 – 900; received February 20, 2007

Dedicated to Dr. Bernard Chevalier on the occasion of his 60th birthday

The structure of CeB_4 has been determined by single crystal X-ray diffraction. The compound crystallizes in the ThB_4 structure type (space group *P*4/*mbm*, a = 7.2034(8), c = 4.1006(5) Å; 270 reflections with $F_o \geq 4\sigma(F_o)$, $R1$ = 0.023, $wR2$ = 0.052). The results of the magnetic and electrical resistivity measurements indicate a strong *f-d* hybridization of the $4f$ electrons of the cerium atom.

Key words: Cerium Boride, Crystal Structure, Magnetic Behaviour, Electrical Resistivity

Introduction

During the study of ternary rare earth metal boride systems, we were faced with uncertainties about the composition and the solid solubility of some binary and ternary systems reported earlier. By investigating the phase equilibria in the Er-Ni-B system the solubility of Ni in ErB_4 had been established [1]. During our investigation of the Ce-B-C ternary system, one of the most frequently observed byproducts was CeB_4. The phase diagram of the binary Ce-B system was previously presented by Spear [2]. Two phases, CeB_6 and CeB_4, were identified in this system. CeB_6 belongs to the CaB_6 structure type [3, 4]. The crystal structure of CeB_4 was only partially studied by X-ray powder diffraction [5].

Studies of the magnetic properties of rare earth metal tetraborides have shown that the compound PrB_4 is ferromagnetic and the compounds with *RE* = Nd, Sm, Gd, Tb, Dy and Ho are antiferromagnetic, while ErB_4 and YbB_4 show a metamagnetic behavior. The elements Ce and Yb exhibit an abnormal valency in the tetraborides [6]. Investigation of the electrical resistivity of REB_4 (*RE* = Y, Nd, Gd, Tb, Dy, Ho, Er and Tm) in the range 300 – 1000 K has confirmed the metallic nature of all these compounds [7].

The structure determination by single crystal X-ray diffraction of CeB_4 as well as investigations of the physical properties (magnetism and electrical resistivity) of a polycrystalline sample are the subject of this paper.

Table 1. Crystallographic data for CeB_4.

Empirical formula	CeB_4
Crystal system	tetragonal
Space group	*P*4/*mbm* (No. 127)
Pearson symbol	tP20
Lattice parameters	
a, Å	7.2034(8)
c, Å	4.1006(5)
Unit cell volume, Å^3	212.78(4)
Calculated density, g cm^{-3}	5.72
Absorption coefficient, cm^{-1}	20.9
Crystal size, mm^3	$0.1 \times 0.07 \times 0.05$
Radiation and wavelength, Å	MoK_α, 0.71069
Refined parameters	19
$2\theta_{max}/(\sin\theta/\lambda)_{max}$	69.56/0.731
hkl Range	$-11 < h < 11$, $-11 < k < 11$, $-6 < l < 6$
Collected reflections	2950
Independent reflections	283
R_{int}	0.040
Reflections with $I_o \geq 2\sigma(I_o)$	270 (R_σ = 0.015)
R_1[a] [$I_o \geq 2\sigma(I_o)$/all data]	0.023/0.026
wR_2[b] [$I_o \geq 2\sigma(I_o)$/all data]	0.053/0.052
Goodness-of-fit on F^2	1.10
Largest diff. peak and hole, e Å^{-3}	1.34/−1.34

[a] $R_1(F) = [\Sigma(|F_o| - |F_c|)]/\Sigma|F_o|$; [b] $wR_2(F^2) = [\Sigma[w(F_o^2 - F_c^2)^2/\Sigma[w(F_o^2)^2]]]^{1/2}$; $[w^{-1} = \sigma^2(F_o)^2 + (0.016P)^2 + 4.5P$, where $P = (F_o^2 + 2F_c^2)/3]$.

Experimental Section

The binary sample CeB_4 was prepared from commercially available pure elements: cerium metal with a claimed purity of 99.99 at. % (Rhône Poulenc, Arizona, USA), crystalline boron powder, purity 99.99 at. % (H. C. Starck, Ger-

0932–0776 / 07 / 0700–0896 $ 06.00 · http://znaturforsch.com

Atom	Site	x	y	z	U_{eq}	U_{11}	U_{22}	U_{33}	U_{12}
Ce	4*g*	0.31445(4)	1/2 + x	0	0.0038(2)	0.0040(2)	U_{11}	0.0035(2)	0.0006(1)
B1	4*e*	0	0	0.202(2)	0.003(1)	0.005(2)	U_{11}	0.004(3)	0
B2	4*h*	0.0880(8)	1/2 + x	1/2	0.001(1)	0.001(1)	0.005(3)	0.012(4)	0.000(2)
B3	8*j*	0.1745(8)	0.0388(8)	1/2	0.004(1)	0.002(2)	0.004(2)	0.006(2)	−0.003(2)

Table 2. Atomic coordinates and displacement parameters[a] (Å^2) for CeB_4.

[a] $U_{23} = U_{13} = 0$.

Table 3. Selected interatomic distances (Å) and bond angles (deg) for CeB_4.

Ce – 4 × Ce	3.7173(4)	B2 – 1 × B2	1.792(8)
Ce – 1 × Ce	3.7783(4)	B2 – 2 × B3	1.746(8)
Ce – 2 × Ce	4.1025(5)	B3 – 2 × Ce	2.798(4)
Ce – 4 × B1	2.757(2)	B3 – 2 × Ce	2.855(4)
Ce – 4 × B2	2.929(4)	B3 – 1 × B2	1.747(7)
Ce – 4 × B3	2.798(4)	B3 – 2 × B1	1.775(7)
Ce – 4 × B3	2.855(4)	B3 – 2 × B3	1.821(8)
B1 – 4 × Ce	2.756(3)	B1–B1–B3	133.5(2)
B1 – 1 × B1	1.66(1)	B3–B1–B3	61.7(3)
B1 – 4 × B3	1.775(7)	B1–B3–B3	59.1(1)
B2 – 4 × Ce	2.929(2)	B3–B2–B2	123.3(3)
B2 – 2 × Ce	3.087(6)	B3–B2–B3	113.4(6)
		B2–B3–B1	136.5(2)

many). Beryllium-copper brass files (Dönges GmbH, Germany) were used for the preparation of Ce powder. Mixtures of powders were compacted in stainless steel dies. The pellets were arc-melted under a purified argon atmosphere on a water-cooled copper hearth. The alloy buttons of *ca.* 1 g were turned over and remelted three times to improve homogeneity. Subsequent annealing was carried out in a high-frequency furnace (TIG-10/300, Hüttinger GmbH, Germany) under a purified argon atmosphere for 24 h at 1770 K.

To check the homogeneity of the sample, X-ray powder diffraction patterns were obtained on a powder diffractometer Stoe STADI P with monochromated Mo$K_{\alpha 1}$ radiation ($7^\circ \leq 2\theta \leq 55^\circ$, step size 0.1°, measurement time per step: 100 s). The lattice parameters of the powder sample and the single crystals agree very well. Elemental germanium (99.9999 %, a_{Ge} = 5.6579 Å) served as the internal standard.

Single-crystal intensity data of CeB_4 were collected at r. t. on a Stoe IPDS-II image plate diffractometer with monochromatized MoK_α radiation in oscillation mode. Single crystal lattice parameters were determined from 5823 reflections in the range $4.0^\circ \leq \theta \leq 35.0^\circ$. All relevant crystallographic information about the data collection and evaluation are listed in Table 1. The starting atomic parameters derived *via* Direct Methods using the program SIR-97 [8] were subsequently refined with full-matrix least-squares methods on F^2 with anisotropic atomic displacements for all atoms using SHELXL-97 [9] within the WINGX program package [10]. The atomic coordinates and displacement parameters are given in Table 2. Selected interatomic distances and bond angles are reported in Table 3. The program DIAMOND was used for the drawing of the crystal structure [11].

Further details of the crystal structure investigation may be obtained from Fachinformationszentrum Karlsruhe, 76344 Eggenstein-Leopoldshafen, Germany (fax: +49-7247-808-666; e-mail: crysdata@fiz-karlsruhe.de, http://www.fiz-informationsdienste.de/en/DB/icsd/depot_anforderung.html) on quoting the deposition number CSD-417745.

Energy dispersive X-ray spectroscopy analysis (EDX) of the polished sample in a scanning electron microscope (Tescan 5130MM with Oxford Si-detector) confirmed the presence of cerium and boron only.

The density measurement of CeB_4 was performed under argon atmosphere in a pycnometer AccuPyc 1330 (Micrometrics GmbH, Germany) and the density was found to be 5.70(3) g cm^{-3} in good agreement with the calculated X-ray density ρ_{calc} = 5.72 g cm^{-3}.

The magnetic properties were studied in the temperature range 1.8 – 800 K by use of a MPMS XL-7 SQUID magnetometer (Quantum Design, Inc.) in external fields up to 7 T. A dc Faraday pendulum magnetometer SUS-10 (A. Paar, Graz, Austria) was applied for measurements in external fields up to 1.3 T in the temperature range 80 K $< T <$ 1100 K.

Measurements of the electrical resistivity were carried out applying a common four-probe technique in the temperature range 4.2 – 300 K. Electrical contacts were made with commercial silver paint (Degussa, Hanau, Germany) and 25 μm gold wire.

Results and Discussion

Structural characterization

The compound CeB_4 belongs to the ThB_4 structure type [5]. Its structure can be described as built up of B_6 octahedra which are linked together in the (001) plane through boron atoms (B2, Table 2) which form B_2 pairs (Fig. 1). The boron octahedra are formed by B(3) squares lying in the z = 1/2 plane which are bicapped by B(1) atoms. The octahedra are close to ideal local O_h symmetry, with intraoctahedral B(1)–B(3) and B(3)–B(3) distances which are quite similar (1.775(7) and 1.821(8) Å, respectively). The B(2) atoms lie in the same z = 1/2 plane as the B(3) squares to which they are connected. As a consequence, being bonded to one other B(2) atom and to two B(3) atoms belonging to two different octahedra, each B(2) atom is tricoordinate. Its bond angles ($2 \times 123.3(3)^\circ$ and $1 \times 113.4(6)^\circ$, see Table 3) indicate sp^2 hybridization. The B(2)–B(3) and B(2)–B(2) distances are 1.746(8) and 1.792(8) Å,

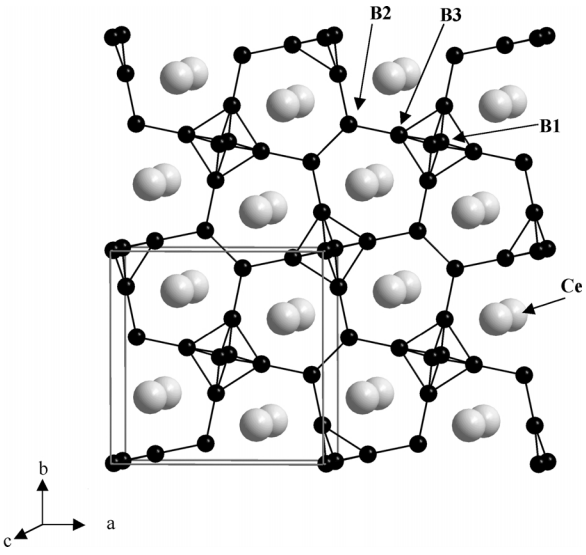

Fig. 1. Crystal structure of CeB_4 as a projection onto the (001) plane.

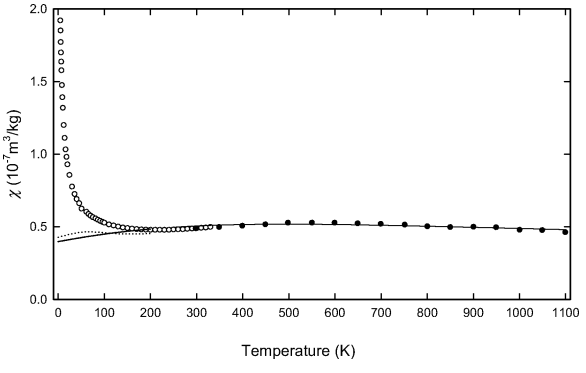

Fig. 2. Magnetic susceptibility measured *versus* temperature for CeB_4. The dotted line represents the data corrected after eq. (1) while the solid line shows those corrected in a least-squares fit employing eqs. (2) and (3).

respectively. The B(2) and B(3) atoms form a planar network at z = 1/2 which can be described as being composed of fused squares and heptagons. However, the entire network of CeB_4 is not 2-dimensional in character since the octahedra are connected along (001) through B(1)–B(1) bonds. These B–B bonds are the shortest in the structure (1.66(1) Å). The boron octahedra lie in cubic voids between Ce atoms, while the B(2) atoms of the B_2 units are located near the centers of face-sharing trigonal prisms of Ce atoms. The metal–boron and boron–boron distances are close to those previously found in isostructural rare earth tetraborides (Table 3) [5, 12 – 18].

Magnetism

The variation of the magnetic susceptibility of CeB_4 with temperature measured up to 1100 K is shown in Fig. 2. The susceptibility is generally very small, of the order of 10^{-9} m^3 per mol Ce atom, and only weakly temperature-dependent. The overall shape of the $\chi(T)$ curve with a characteristic broad maximum occurring at elevated temperatures is reminiscent of an intermediate-valence (IV) system. At low temperatures we observe an increase of the susceptibility in contrast to the expected tendency for an IV compound to reach a constant value $\chi(0)$ at T = 0 K. Such a behavior is commonly attributed to the presence of small amounts of impurities, such as oxides of cerium, *etc*. [19, 20]. Following a procedure employed by Béal-Monod and Lawrence [19] the measured low temperature susceptibility can be expressed as

$$\chi(T \to 0) = \chi(0) + \frac{C_{\mathrm{imp}}}{T} \qquad (1)$$

where $\chi(0)$ denotes the intrinsic susceptibility at T = 0 K and C_{imp} is the Curie constant of magnetic impurity moments. Assuming stable Ce^{3+} ions as the major impurity component, their contribution is defined as $n = C_{\mathrm{imp}}/C$, where C = 0.807 emu mol^{-1} K^{-1} is the Curie constant of free Ce^{3+} ions. Fitting our data for $T < 100$ K to eq. (1) yielded $\chi(0) = 7.1 \times 10^{-4}$ emu per mol Ce atom and $n = 13.6 \times 10^{-3}$ Ce atom mol^{-1}. The measured susceptibility data were corrected for impurities by subtracting the term nC/T from the experimental data. The so-corrected $\chi(T)$ data are shown in Fig. 2 as a dotted line.

In addition, we tried to describe the features of an IV system within the scope of the interconfiguration fluctuation (ICF) model developed by Sales and Wohlleben [21]. The temperature dependence of the magnetic susceptibility of an IV cerium compound is given by

$$\chi(T) = \frac{N\mu_{\mathrm{eff}}^2[1-\nu(T)]}{3k_{\mathrm{B}}(T-T_{\mathrm{SF}})} + \chi_0 \qquad (2)$$

where μ_{eff} = 2.54 μ_{B} is the effective moment of the cerium $4f^1$ state, T_{SF} denotes a characteristic temperature associated with fluctuations between the $4f^1$ and $4f^0$ states due to interactions with conduction electrons, while $\nu(T)$ stands for the mean occupation of the ground state. This fractional occupation is temper-

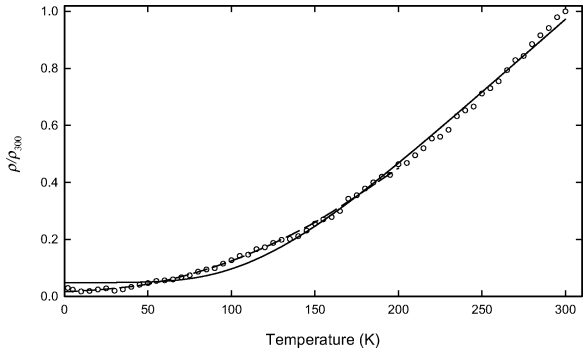

Fig. 3. Electrical resistivity *vs.* temperature for CeB_4. The solid line shows the fit applying eq. (4) and the dashed line that applying eq. (5).

ature and energy dependent *via* the relation

$$\nu(T) = \frac{1}{1+6\exp[-E_{ex}/k_B(T+T_{SF})]} \qquad (3)$$

where E_{ex} is the energy difference between the $4f^1$ and $4f^0$ states and χ_0 is a constant term accounting for core diamagnetism and Pauli paramagnetism. The magnetic behavior of CeB_4 observed for $T > 150$ K is described quite well by this ICF model. The least-squares fit of the experimental $\chi(T)$ data is presented in Fig. 2 as the solid line. The fitting parameters are: $E_{ex}/k_B = 1930$ K, $T_{SF} = 522$ K and $\chi_0 = 3.8 \times 10^{-4}$ emu per mol Ce atom. These parameters indicate a decrease of the cerium valence from 3.7 at 200 K down to 3.4 at 900 K. Finally, it should be noted that the nonmagnetic ground state for this compound can be deduced from the small magnitude of the almost temperature independent susceptibility, but also from the large values of T_{SF} and E_{ex} derived above.

Electrical resistivity

The experimental data of the electrical resistivity of CeB_4 are presented in Fig. 3. The $\rho(T)$ curve is reminiscent of the behavior of IV materials [22]. The result of the magnetic measurements (above) led to the assumption that the cerium atom is practically nonmagnetic below r. t. Hence, based on Matthiesen's rule, the temperature dependence of the resistivity of our compound, due to the overall shape of the resistivity plot of a nonmagnetic metal, can be described by the Bloch-Grüneisen relation [23]

$$\rho(T) = \rho_0 + 4R\Theta_D\left(\frac{T}{\Theta_D}\right)^5 \int_0^{\Theta_D/T} \frac{x^5 dx}{(e^x-1)(1-e^{-x})} \qquad (4)$$

where ρ_0 is the temperature independent residual resistivity and the second term accounts for the electron-phonon scattering process. The temperature-independent coefficient R in eq. (4) is directly related to the strength of the electron-phonon interactions, whereas the symbol Θ_D stands for the Debye temperature. A least-squares fit according to eq. (4) gave the following values: $\rho_0/\rho_{300} = 0.0049$, $R' = 0.00436$ K^{-1} and $\Theta_D = 775$ K. The fit is shown in Fig. 3 as the solid line.

Alternatively, according to the paramagnon picture of such intermediate-valence systems the resistivity should obey a T^2 dependence characteristic of a Fermi liquid at low temperature [20]. Indeed, as shown in Fig. 3 by the dashed line, the relative resistivity can be described very well by the expression

$$\rho(T) = \rho_0 + AT^2 \qquad (5)$$

for the whole temperature range below $T = 130$ K with the following parameters: residual resistivity $\rho_0/\rho_{300} = 0.016$ and $A = 1.084 \times 10^{-5}$ K^{-2}.

Summary

The crystal structure of CeB_4 has been verified (ThB_4 type of structure, space group *P*4/*mbm*) and refined from single crystal data. The magnetic and electrical properties of CeB_4 prove the intermediate valence state of Ce as a consequence of a strong *f-d* hybridization of the $4f$ orbitals.

[1] V. Babizhetskyy, I. Veremchuk, N. Chaban, Yu. Kuz'ma, *J. Alloys Compd.* **2004**, *377*, 117.
[2] K. E. Spear, Phase diagrams, *Mater. Sci. Technol*. **1976**, *4*, 91.
[3] S. Sato, *J. Magn. Magn. Mater*. **1985**, *52*, 310.
[4] P. Blum, F. Bertraut, *Acta Crystallogr*. **1954**, *7*, 81.
[5] A. Zalkin, D. H. Templeton, *Acta Crystallogr*. **1953**, *6*, 269.
[6] K. H. J. Buschow, J. H. N. Creyghton, *J. Chem. Phys*. **1972**, *57*, 3910.
[7] E. N. Severyanina, E. M. Dudnik, Yu. B. Paterno, *Poroshk. Metallugiya* **1974**, *10*, 85.
[8] A. Altomare, M. C. Burla, M. Camalli, B. Carroccini, G. L. Cascarano, C. Giacovazzo, A. Guagliardi, A. G. Moliterni, G. Polidori, R. Rizzi, *J. Appl. Crystallogr*. **1999**, *32*, 115.

[9] G. M. Sheldrick, SHELXL-97, Program for the Refinement of Crystal Structures, University of Göttingen, Göttingen (Germany) **1997**.
[10] L. J. Farrugia, WINGX, version 1.64.05, *J. Appl. Crystallogr.* **1999**, *32*, 837.
[11] K. Brandenburg, DIAMOND (version 2.1e), Crystal and Molecular Structure Visualization, Crystal Impact GbR, Bonn (Germany) **1996 – 2001**.
[12] R. F. Giese Jr., V. I. Matkovich, J. Economy, *Z. Kristallogr.* **1965**, *122*, 423.
[13] K. Kato, I. Kawada, C. Oshima, S. Kawai, *Z. Kristallogr.* **1974**, *B30*, 2933.
[14] P. Salamakha, A. P. Gonçalves, O. Sologub, M. Almeida, *J. Alloys Compd.* **2001**, *316*, L4.
[15] L. V. Zavalii, V. A. Bruskov, Yu. B. Kuz'ma, *Inorg. Mater.* **1988**, *24*, 1350.
[16] M. T. Garland, J. P. Wiff, J. Bauer, R. Guerin, J. Y. Saillard, *Solid State Sci.* **2003**, *5*, 705.
[17] F. Elf, W. Schäfer, G. Will, J. Etourneau, *Solid State Commun.* **1981**, *40*, 579.
[18] W. Schäfer, G. Will, *Z. Kristallogr.* **1976**, *144*, 217.
[19] M. T. Béal-Monod, J. M. Lawrence, *Phys. Rev. B* **1980**, *21*, 5400.
[20] J. M. Lawrence, P. S. Riseborough, R. D. Parks, *Rep. Prog. Phys.* **1981**, *44*, 1.
[21] B. C. Sales, D. K. Wohlleben, *Phys. Rev. Lett.* **1975**, *35*, 1240.
[22] D. K. Wohlleben, B. Wittershagen, *Adv. Phys.* **1985**, *34*, 403.
[23] G. Grimvall, *The Electron-Phonon Interaction in Metals*, North-Holland, Amsterdam (The Netherlands) **1981**.